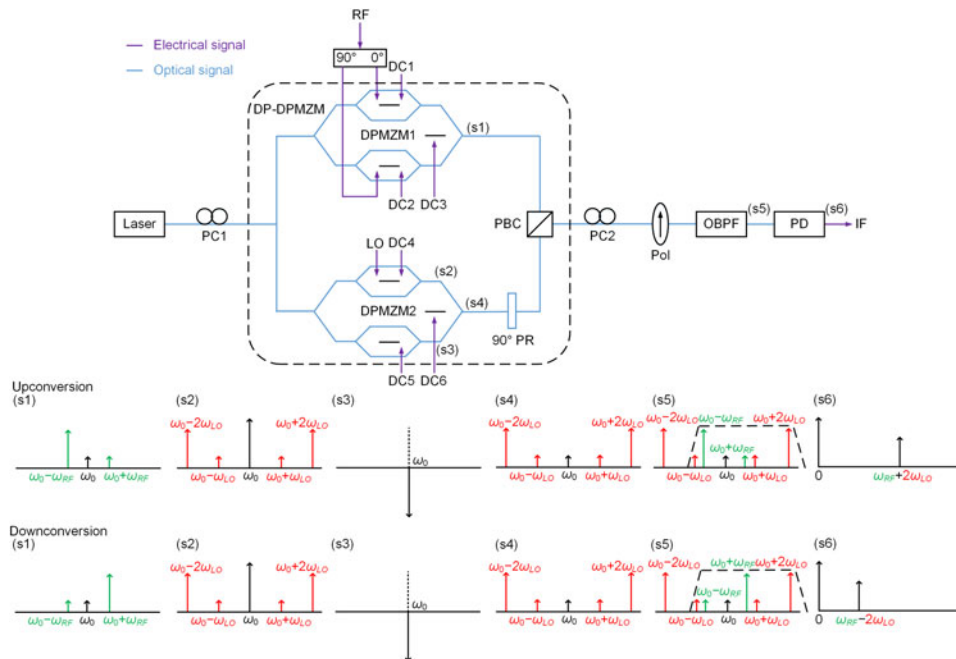


# A Microwave Photonic Mixer Using a Frequency-Doubled Local Oscillator

Volume 10, Number 3, June 2018

Jingnan Li  
Yunxin Wang  
Dayong Wang  
Tao Zhou  
Jiahao Xu  
Xin Zhong  
Feng Yang  
Dengcai Yang  
Lu Rong



DOI: 10.1109/JPHOT.2018.2838587

1943-0655 © 2018 CCBY

# A Microwave Photonic Mixer Using a Frequency-Doubled Local Oscillator

Jingnan Li <sup>1</sup>, Yunxin Wang <sup>1</sup>, Dayong Wang,<sup>1</sup> Tao Zhou,<sup>2</sup>  
Jiahao Xu,<sup>1</sup> Xin Zhong,<sup>2</sup> Feng Yang,<sup>1</sup> Dengcai Yang,<sup>1</sup> and Lu Rong<sup>1</sup>

<sup>1</sup>College of Applied Sciences, Beijing University of Technology, Beijing 100124, China, and also with the Beijing Engineering Research Center of Precision Measurement Technology and Instruments, Beijing University of Technology, Beijing 100124, China

<sup>2</sup>Science and Technology on Electronic Information Control Laboratory, Chengdu 610036, China

DOI:10.1109/JPHOT.2018.2838587

This work is licensed under a Creative Commons Attribution 3.0 License. For more information, see <http://creativecommons.org/licenses/by/3.0/>

Manuscript received April 4, 2018; revised May 14, 2018; accepted May 16, 2018. Date of publication May 21, 2018; date of current version June 12, 2018. This work was supported in part by the National Natural Science Foundation of China under Grants 61771438, 51477028, and 61372061, in part by the Beijing Municipal Natural Science Foundation (4162015), and in part by the Importation and Development of High-Caliber Talents Project of Beijing Municipal Institutions under Grant CIT&TCD201504020. Corresponding authors: Dayong Wang and Yunxin Wang (e-mail: wdyong@bjut.edu.cn; yxwang@bjut.edu.cn).

**Abstract:** A microwave photonic mixer based on a frequency-doubled local oscillator (LO) is proposed. The carrier-suppressed single-sideband (CS-SSB) modulation of the  $-$ first-order radio frequency (RF) and  $+$ second-order LO sidebands can be generated by using a dual-polarization dual-parallel Mach-Zehnder modulator (DP-DPMZM), an electrical  $90^\circ$  hybrid coupler, and an optical bandpass filter. The upconverted intermediate frequency (IF) signal with the frequency of  $\omega_{RF} + 2\omega_{LO}$  is output by frequency beat at a photodetector. Meanwhile, the  $-$ first-order RF sideband can be easily changed to  $+$ first-order RF sideband by adjusting one dc bias voltage of the DP-DPMZM. The downconverted IF signal with the frequency of  $\omega_{RF} - 2\omega_{LO}$  is obtained correspondingly. The experimental results show that the spur suppression ratios of upconverted and downconverted IF signal are 19.0 dB and 25.5 dB, respectively. The spurious-free dynamic range of the proposed mixer is  $96.5 \text{ dB}\cdot\text{Hz}^{2/3}$ . The output electrical spectrums are pure owing to the optimal design of the CS-SSB modulation. The proposed mixer reduces the frequency requirement of LO signal since the second-order LO single sideband is used, and the upconversion and downconversion can be switched to each other by a simple electrical operation.

**Index Terms:** Fiber optics links and subsystems, radio frequency photonics, analog optical signal processing.

## 1. Introduction

Owing to the inherent characteristics such as broad bandwidth, low loss and immunity to electromagnetic interference (EMI), microwave photonic links have become more attractive and have been applied in radio over fiber (RoF) system, phased-array beamforming and high-speed signal processing, etc. [1]–[3].

A frequency mixer is a very important component of transceiver to implement frequency conversion for the radio frequency (RF) signal with the frequency of  $\omega_{RF}$  by using a corresponding local oscillator (LO) signal with the frequency of  $\omega_{LO}$  [4]. For the conventional electrical mixers and most of the microwave photonic mixers [5]–[16], the frequency of the generated intermediate frequency (IF) signal is  $\omega_{RF} \pm \omega_{LO}$ . Two Mach-Zehnder modulators (MZM) in series can achieve frequency

downconversion based on the double-sideband (DSB) modulation [5]. The desired IF signal generated by a photodetector (PD) is disturbed by lots of mixing spurs. In order to suppress the LO and RF spurs, the carrier-suppressed double-sideband (CS-DSB) modulation is applied to reduce the influence of the useless optical carrier [6]–[10]. The optical carrier can be removed by the stimulated Brillouin scattering (SBS) technique [6], Sagnac loop interferometer [7] and fiber Bragg grating [8]. Besides, some integrated modulators, such as dual-drive MZM (DMZM) or dual-parallel MZM (DPMZM), can be operated at minimum transmission point to suppress the optical carrier directly [9], [10]. Although the RF and LO leakages are greatly suppressed, the harmonic spurs, such as  $2\omega_{RF}$  and  $2\omega_{LO}$ , are still inevitable which are produced by frequency beat of  $\pm 1$ st-order RF/LO sidebands. Therefore, the carrier-suppressed single-sideband modulation (CS-SSB) based microwave photonic mixers are presented to further suppress these mixing spurs [11]–[15]. Optical bandpass filter (OBPF) can be commonly used to filter out one of the sidebands [11]–[13]. Besides, a DPMZM with an electrical  $90^\circ$  hybrid coupler can be also optimized to achieve CS-SSB modulation for frequency mixing [14], [15]. Recently, these two methods are combined to realize ultra-wideband CS-SSB modulation for downconversion by using a DPMZM, an electrical  $90^\circ$  hybrid coupler and an OBPF [16]. How to improve the purity of microwave photonic frequency mixer has attracted more attention. As shown in the Refs [11]–[16], it has been demonstrated that the CS-SSB modulation is a good choice for microwave photonic mixers to suppress the spurs in electrical domain.

On the other hand, the transmitted or received microwave signals have been raised to millimeter wave band as the increasing of frequency in microwave communication. To adapt the higher working frequency, the LO frequency has to be improved correspondingly for the traditional frequency mixer. Fortunately, the LO signal with lower frequency can be still optimized to realize high-frequency mixer profiting from the great flexibility of microwave photonics. Several microwave photonic mixers have been proposed based on higher-order sideband of LO signal [17]–[20]. In reference [17], a DPMZM is used to implement upconversion with frequency doubling. Although the optical carrier is suppressed, the harmonic mixing spurs produced by frequency beat between positive and negative sidebands are unavoidable. The cascaded structure of a MZM and a DPMZM realizes frequency doubled upconversion while compensating the chromatic-dispersion-induced power fading [18]. In addition, three MZMs in series are applied to realize the upconversion with frequency quadrupling for RoF link [19]. The useless sidebands of optical spectrums are not well suppressed in references [18], [19], thus the interested IF signal with lots of mixing spurs is generated in electrical spectrums. Except the frequency upconversion, the frequency doubled method can also be applied in downconversion system [20]. The sub-harmonic frequency downconversion with phase shifting can be achieved by using a dual-polarization DPMZM (DP-DPMZM) and an OBPF. The  $+1$ st-order RF sideband and  $+2$ nd-order LO sideband are both retained by OBPF to generate IF signal at PD, which reduce the frequency requirement of LO signal in downconverter.

In this paper, a microwave photonic mixer using a frequency doubled LO signal is proposed based on CS-SSB modulation. The first sub-DPMZM of DP-DPMZM is driven by the RF signal through an electrical  $90^\circ$  hybrid coupler. The CS-SSB modulation of the  $-1$ st-order RF sideband is generated. The LO signal only modulates the upper sub-MZM of the second sub-DPMZM, and the CS-DSB modulation of the 2nd-order LO sidebands are obtained by controlling three DC bias voltages. Owing to a  $90^\circ$  polarization rotator (PR) and a polarization beam combiner (PBC), the  $-1$ st-order RF sideband and the  $\pm 2$ nd-order LO sidebands are output with orthogonal polarization state. A polarization controller (PC) and a polarizer (Pol) in series are used to project the RF and LO optical signals to the linear polarization states. An OBPF is applied to achieve the CS-SSB modulation of the  $+2$ nd-order LO sideband. Thus, the  $-1$ st-order RF and  $+2$ nd-order LO sidebands are obtained after the OBPF. The upconverted IF signal with the frequency of  $\omega_{RF} + 2\omega_{LO}$  can be obtained by frequency beat at PD. Besides, the CS-SSB modulation can be easily changed from  $-1$ st to  $+1$ st-order RF sideband by tuning the DC bias voltage of the parent MZM in the first sub-DPMZM. In this case, the downconverted IF signal with the frequency of  $\omega_{RF} - 2\omega_{LO}$  can be acquired after PD. The proposed microwave photonic mixer is theoretically analyzed and experimentally demonstrated.

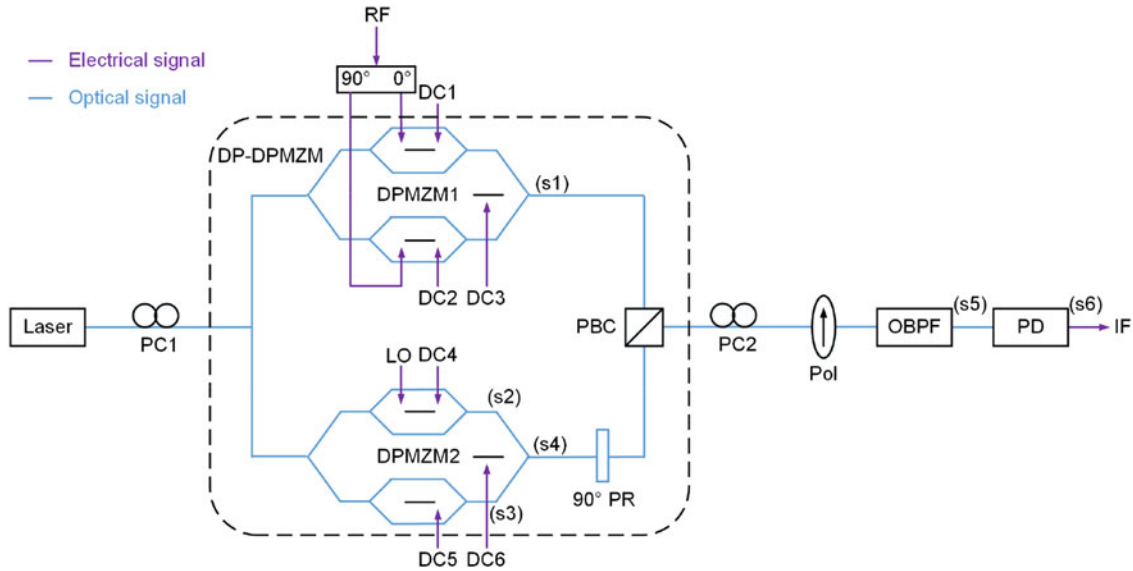


Fig. 1. Schematic diagram of the proposed microwave photonic mixer.

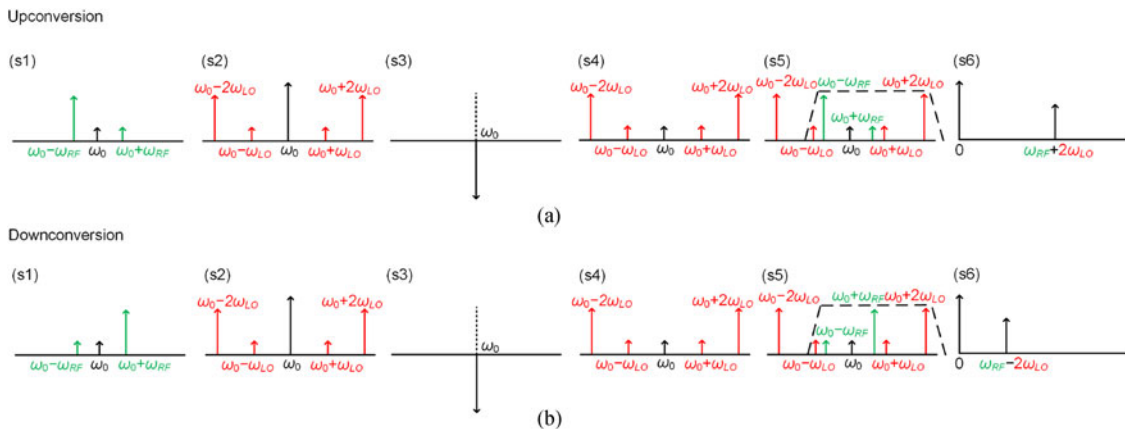


Fig. 2. Corresponding optical and electrical spectrums at different locations in Fig. 1. (a) Upconversion. (b) Downconversion.

The upconverted or downconverted IF signal is quite pure due to the optimal design of CS-SSB modulation. The spur suppression ratios of upconverted and downconverted IF signal are 19.0 dB and 25.5 dB, respectively. The spurious-free dynamic range (SFDR) of system is  $96.5 \text{ dB} \cdot \text{Hz}^{2/3}$ . The presented approach greatly reduces the frequency requirement of LO signal, and the upconversion mode can be switched to the downconversion mode by a simple electrical operation of one DC bias.

## 2. Topology and Operation Principle

The schematic diagram of the proposed microwave photonic mixer is shown in Fig. 1. The system consists of a laser source, a DP-DPMZM, an electrical  $90^\circ$  hybrid coupler, two PCs, a Pol, an OBPF and a PD. Fig. 2 describes the corresponding optical and electrical spectrums at different locations in Fig. 1 for both upconversion and downconversion modes.

A continuous lightwave as the optical carrier is launched into a DP-DPMZM after a PC. The DP-DPMZM is comprised of two sub-DPMZMs with parallel structure, a  $90^\circ$  PR and a PBC. The

optical carrier is equally split into two sub-DPMZMs. The RF signal is input to an electrical 90° hybrid coupler which outputs two signals with the same amplitude and quadrature phase, and then modulate the two sub-MZMs of the DPMZM1. The LO signal only modulates the upper sub-MZM in DPMZM2. The optical field of two sub-DPMZMs can be described by

$$E_{DPMZM1}(t) = \frac{\sqrt{2}}{8} \sqrt{P_0} \sqrt{L_{DPMZM}} e^{j\omega_0 t} \cdot \left\{ \begin{array}{l} \left[ \begin{array}{l} e^{j(m_{RF} \cos \omega_{RF} t + \theta_1/2)} \\ + e^{-j(m_{RF} \cos \omega_{RF} t + \theta_1/2)} \end{array} \right] e^{j\theta_3/2} \\ + \left[ \begin{array}{l} e^{j(m_{RF} \cos(\omega_{RF} t + \pi/2) + \theta_2/2)} \\ + e^{-j(m_{RF} \cos(\omega_{RF} t + \pi/2) + \theta_2/2)} \end{array} \right] e^{-j\theta_3/2} \end{array} \right\} \quad (1)$$

$$E_{DPMZM2}(t) = \frac{\sqrt{2}}{8} \sqrt{P_0} \sqrt{L_{DPMZM}} e^{j\omega_0 t} \cdot \left\{ \begin{array}{l} \left[ \begin{array}{l} e^{j(m_{LO} \cos \omega_{LO} t + \theta_4/2)} \\ + e^{-j(m_{LO} \cos \omega_{LO} t + \theta_4/2)} \end{array} \right] e^{j\theta_6/2} \\ + \left[ e^{j\theta_5/2} + e^{-j\theta_5/2} \right] e^{-j\theta_6/2} \end{array} \right\} \quad (2)$$

where  $P_0$  and  $\omega_0$  are the power and the angular frequency of optical carrier, respectively.  $L_{DPMZM}$  is the insertion loss of the DPMZM.  $\omega_{RF}$  and  $\omega_{LO}$  are the angular frequencies of RF and LO signals.  $m_{RF} = \pi V_{RF}/V_\pi$  and  $m_{LO} = \pi V_{LO}/V_\pi$  are the modulation depths of the sub-MZMs in two DPMZMs.  $V_{DCn}$  ( $n = 1, 2 \dots 6$ ) is the DC bias voltage and  $V_\pi$  is the half-wave voltage of the DPMZM.  $\theta_n = \pi V_{DCn}/V_\pi$  is the phase difference between two arms induced by the corresponding DC bias voltage.

In order to obtain CS-SSB modulation of the  $-1$ st-order RF sideband, the two sub-MZMs of DPMZM1 are biased at the minimum transmission points to achieve the optical carrier suppression, where  $\theta_1 = \theta_2 = \pi$ , and  $\theta_3 = -\pi/2$  should be satisfied [21]. Furthermore, when the  $\theta_3$  is changed from  $-\pi/2$  to  $\pi/2$ , the  $-1$ st-order CS-SSB modulation of RF sideband can be switched to the  $+1$ st-order CS-SSB modulation. The corresponding spectrums are shown in Fig. 2(a)-(s1) and (b)-(s1). Therefore, the CS-SSB modulation of RF signal can be output from DPMZM1. To realize DSB modulation of LO signal, the upper sub-MZM of DPMZM2 works at the maximum transmission point by setting  $\theta_4 = 2\pi$ . Through controlling the DC bias voltages  $V_{DC5}$  and  $V_{DC6}$  to satisfy  $\theta_5 = 2 \arccos J_0(m_{LO})$  and  $\theta_6 = 2\pi$ , the optical carrier from DPMZM2 can be suppressed [20]. Thus, a CS-DSB modulation of the 2nd-order LO sidebands is obtained. Then, a 90° PR is used to rotate the polarization state of the output optical signals from DPMZM2. Next, the optical signals of the CS-SSB modulation of the 1st-order RF sideband and the CS-DSB modulation of the 2nd-order LO sidebands with orthogonal polarization states are combined and output after a PBC.

Here, we firstly discuss the upconversion mode where the CS-SSB modulation of the  $-1$ st-order RF sideband is obtained by setting  $\theta_3 = -\pi/2$ . The output optical field of DP-DPMZM with orthogonal polarization states can be expressed as

$$E_{DP-DPMZM}(t) = \begin{bmatrix} E_X(t) \\ E_Y(t) \end{bmatrix} = \begin{bmatrix} \frac{\sqrt{2}}{2} \sqrt{P_0} \sqrt{L_{DPMZM}} e^{j\omega_0 t} \left[ J_1(m_{RF}) e^{-j(\omega_{RF} t + \pi/4)} \right] \\ \frac{\sqrt{2}}{4} \sqrt{P_0} \sqrt{L_{DPMZM}} e^{j\omega_0 t} \left[ \begin{array}{l} J_2(m_{LO}) e^{j2\omega_{LO} t} \\ + J_2(m_{LO}) e^{-j2\omega_{LO} t} \end{array} \right] \end{bmatrix} \quad (3)$$

where  $J_n(\cdot)$  is the  $n$ th-order Bessel function of the first kind, and here the higher order ( $n \geq 3$ ) sidebands are ignored. The orthogonally polarized optical signals are projected onto a linear

polarization state by combining a PC and a Pol with an angle of 45°. Thus, the optical field after polarizer is

$$E_{Pol}(t) = \frac{1}{2} \sqrt{P_0} \sqrt{L_{DPMZM}} e^{j\omega_0 t} \cdot \left\{ J_1(m_{RF}) e^{-j(\omega_{RF} t + \pi/4)} + \frac{1}{2} \left[ \begin{array}{l} J_2(m_{LO}) e^{j2\omega_{LO} t} \\ + J_2(m_{LO}) e^{-j2\omega_{LO} t} \end{array} \right] \right\} \quad (4)$$

Then, the OBPF is used to filter out the -2nd-order LO sideband as shown in Fig. 2(a)-(s5). Thus the CS-SSB modulation of the +2nd-order LO sideband is realized. The output optical signals of OBPF can be written as

$$E_{OBPF}(t) = \frac{1}{2} \sqrt{P_0} \sqrt{L_{DPMZM}} \sqrt{L_{OBPF}} e^{j\omega_0 t} \cdot \left\{ J_1(m_{RF}) e^{-j(\omega_{RF} t + \pi/4)} + \frac{1}{2} J_2(m_{LO}) e^{j2\omega_{LO} t} \right\} \quad (5)$$

where  $L_{OBPF}$  is the insertion loss of the OBPF. We can see that the CS-SSB modulation of RF and LO signals ensures the purity of optical spectrum. The output optical signals of the OBPF frequency beat at the PD to perform optical-to-electrical conversion, and the output photocurrent of PD is

$$\begin{aligned} i_{IF}(t) &= \Re E_{OBPF}(t) \cdot E_{OBPF}^*(t) \\ &= \frac{1}{4} \Re P_0 L_{DPMZM} L_{OBPF} J_1(m_{RF}) J_2(m_{LO}) \\ &\quad \cdot \cos \left[ (\omega_{RF} + 2\omega_{LO})t + \frac{\pi}{4} \right] \end{aligned} \quad (6)$$

where  $\Re$  is the responsivity of the PD. The IF signal with the frequency of  $\omega_{RF} + 2\omega_{LO}$  can be detected. As can be seen, the upconverted IF signal with frequency doubling can be obtained.

To switch to the downconversion mode,  $V_{DC3}$  should be adjusted to satisfy  $\theta_3 = \pi/2$ , and the CS-SSB modulation of the +1st-order RF sideband can be produced. The OBPF is used to retain the +2nd-order LO sideband and the +1st-order RF sideband as shown in Fig. 2(b)-(s5). The output optical signals of OBPF can also remain a good purity and can be written as

$$E_{OBPF}(t) = \frac{1}{2} \sqrt{P_0} \sqrt{L_{DPMZM}} \sqrt{L_{OBPF}} e^{j\omega_0 t} \left\{ \begin{array}{l} J_1(m_{RF}) e^{j(\omega_{RF} t + \pi/4)} \\ + \frac{1}{2} J_2(m_{LO}) e^{j2\omega_{LO} t} \end{array} \right\} \quad (7)$$

The IF signal is detected by PD and the output photocurrent is

$$\begin{aligned} i_{IF}(t) &= \frac{1}{4} \Re P_0 L_{DPMZM} L_{OBPF} J_1(m_{RF}) J_2(m_{LO}) \\ &\quad \cdot \cos \left[ (\omega_{RF} - 2\omega_{LO})t + \frac{\pi}{4} \right] \end{aligned} \quad (8)$$

It is clearly observed that the downconverted IF signal with the frequency of  $\omega_{RF} - 2\omega_{LO}$  can be generated. In conclusion, the frequency up and downconversion can be achieved with frequency doubling of the LO signal, which can reduce the frequency requirement of LO signal for transmitter and receiver. Besides, the frequency upconversion can be easily switched to the downconversion mode by controlling a DC bias voltage  $V_{DC3}$  of DP-DPMZM.

### 3. Experimental Results

A proof-of-concept experiment based on the schematic diagram shown in Fig. 1 is carried out. The continuous optical carrier is output from a distributed feedback (DFB) laser. The wavelength is 1550.09 nm and the power is 17.6 dBm. The optical carrier is launched to a commercial DP-DPMZM

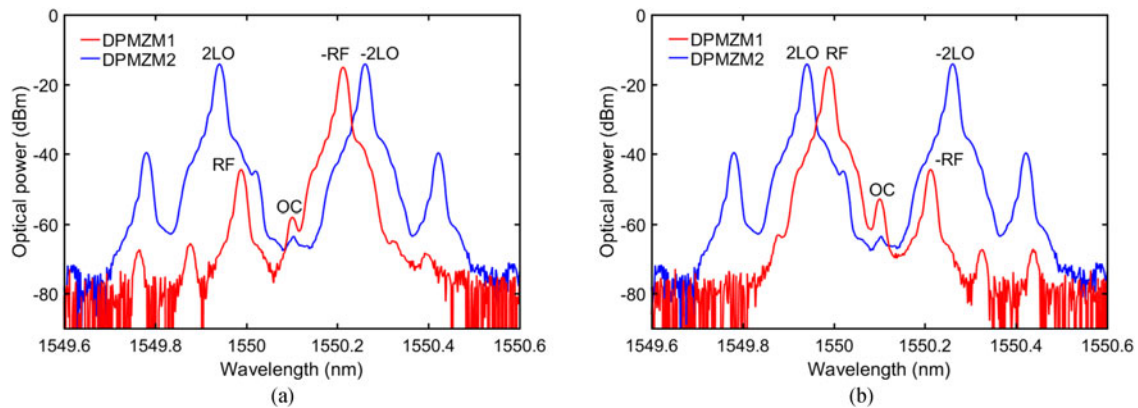


Fig. 3. The optical spectrums of DPMZM1 and DPMZM2 in (a) upconversion and (b) downconversion.

(Fujitsu FTM7977HQA). The RF signal is sent to an electrical  $90^\circ$  hybrid coupler (Marki Microwave QH-0226). Two microwave signals with the same amplitude and quadrature phase are output. These signals are injected into two sub-MZMs of the DPMZM1. Two sub-MZMs in the DPMZM1 are both biased at the minimum transmission points to realize carrier suppression. The  $V_{DC1}$  and  $V_{DC2}$  are set to 16.1 V and 13.5 V, respectively. The  $V_{DC3}$  is adjusted to 21.5 V for the CS-SSB modulation of the  $-1$ st-order RF sideband (upconversion mode) or 14.8 V for that of the  $+1$ st-order RF sideband (downconversion mode). The upper sub-MZM of DPMZM2 is only modulated by the LO signal, which operates at the maximum transmission point to achieve DSB modulation of the 2nd-order LO sidebands where the  $V_{DC4}$  is tuned to 12.2 V. By adjusting the  $V_{DC5}$  to 12.8 V and  $V_{DC6}$  to 1.8 V, the CS-DSB modulation of the 2nd-order LO sidebands is output from DPMZM2. Thus, the CS-SSB modulation of the 1st-order RF sideband and the CS-DSB modulation of the 2nd-order LO sidebands are output from DP-DPMZM with orthogonal polarization directions due to a  $90^\circ$  PR and a PBC. The PC and Pol in series, as a  $45^\circ$  polarizer, project the two orthogonally polarized optical signals onto the same polarization state. The OBPF is applied to remove the  $-2$ nd-order LO sideband to realize the CS-SSB of the  $+2$ nd-order LO sideband, and the higher-order LO sidebands are also suppressed. An erbium-doped fiber amplifier (EDFA) is used to compensate the insertion loss of DP-DPMZM and OBPF. The output optical power of EDFA maintains at 1.6 dBm which works at automatic power control (APC) mode. Finally, the optical signal is sent to a PD (FINISAR, XPDV2120R) to implement optical-to-electrical conversion. The bandwidth and responsivity of the PD are 50 GHz and 0.65 A/W, respectively. The IF signal is obtained by using frequency doubled LO signal.

To test the performance of the CS-SSB modulation of the 1st-order RF sideband and the CS-DSB modulation of the 2nd-order LO sidebands, the optical spectrums are analyzed by an optical spectrum analyzer (OSA, Yokogawa AQ6370C). Through changing the polarization angle between the optical signals and polarizer by a PC, the output optical signals from DPMZM1 and DPMZM2 with orthogonal polarization states can be obtained, respectively. The power and frequency of LO signal are 19 dBm and 10 GHz, respectively. The power of RF signal is 10 dBm, and its frequency is 14 GHz. The output optical spectrums of DPMZM1 and DPMZM2 are measured and the results are shown in Fig. 3. For the upconversion mode as described in Fig. 3(a). The sideband suppression ratio of  $-1$ st to  $+1$ st-order RF sidebands is 29.5 dB, and the carrier suppression ratio of  $-1$ st-order RF sideband is 43.0 dB. The carrier suppression ratio of the 2nd-order LO sideband is 49.3 dB. When changing the  $V_{DC3}$  of the DP-DPMZM from 21.5 V to 14.8 V, the downconversion mode is achieved and the spectrums are shown in Fig. 3(b). The sideband suppression ratio of  $+1$ st to  $-1$ st-order RF sideband is also 29.5 dB and the carrier suppression ratio of the  $+1$ st-order RF sideband is 38.0 dB. The carrier suppression ratio of the 2nd-order LO sideband is also 49.3 dB since the DPMZM2 is unchanged during mode switch. For both the upconversion and

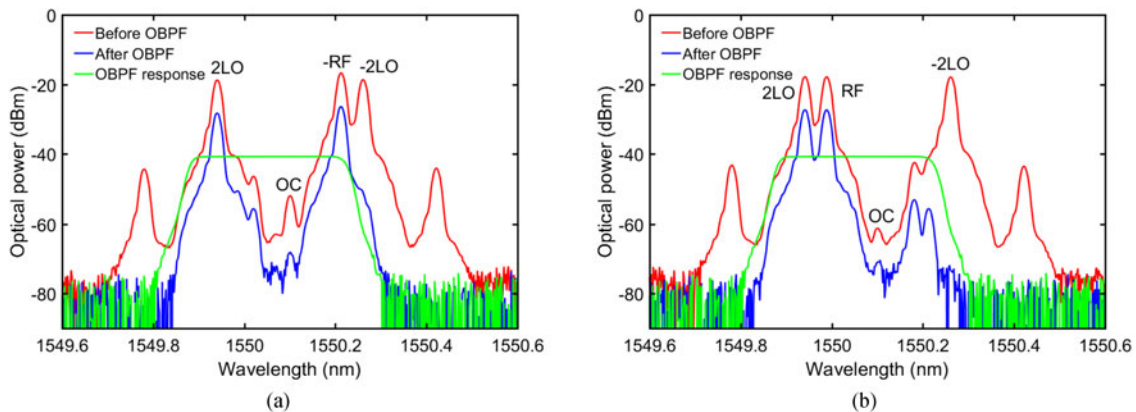


Fig. 4. The optical spectrums before and after OBPF in (a) upconversion and (b) downconversion.

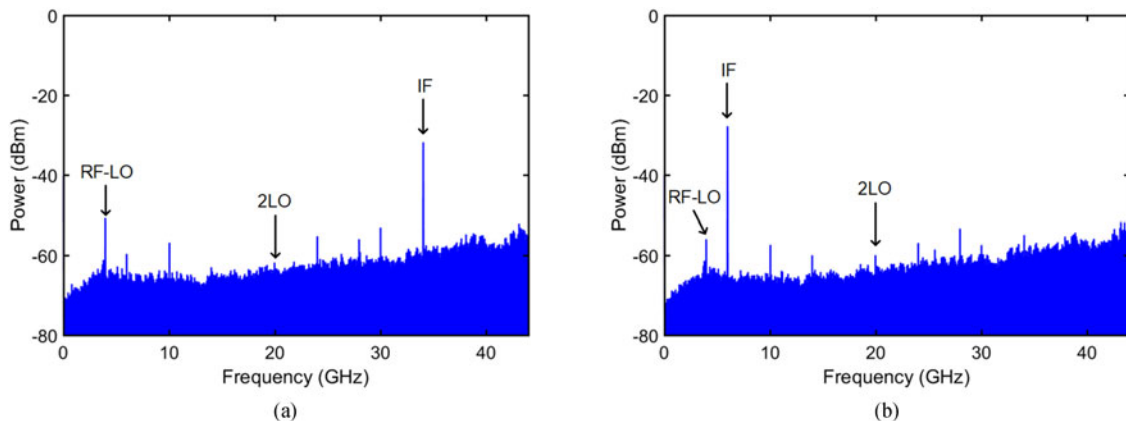


Fig. 5. The electrical spectrums of the proposed microwave photonic mixer in (a) upconversion and (b) downconversion.

downconversion modes, it is demonstrated that the CS-SSB modulation of the 1st-order RF sideband and the CS-DSB modulation of the 2nd-order LO sidebands are well implemented with a high suppression ratio.

Then, the performance of the CS-SSB modulation of the +2nd-order LO sideband is further analyzed. By changing the angle between the optical signals and Pol to  $45^\circ$  through a PC, the output optical signals from DPMZM1 and DPMZM2 with orthogonal polarization directions are projected onto the same polarization direction. The OBPF is applied to remove the -2nd-order and other higher-order LO sidebands to achieve the CS-SSB modulation of the +2nd-order LO sideband. The optical spectrums before and after OBPF are measured and shown in Fig. 4. The response of OBPF is measured by using a broadband optical source. In the upconversion case as shown in Fig. 4(a), the +2nd-order LO and the -1st-order RF sidebands are retained. In the downconversion case, we can see that the +2nd-order LO and the +1st-order RF sidebands are left as depicted in Fig. 4(b). The -2nd-order LO sideband and other useless optical signals out of the passband of OBPF are suppressed under the noise floor in both upconversion and downconversion modes. It is clearly seen that the CS-SSB modulations of the 1st-order RF and the +2nd-order LO sidebands are implemented successfully, all of which ensure a high purity of optical spectrums.

Next, the electrical spectrum is analyzed under the same experimental condition. The output electrical signal after PD is measured by an electrical spectrum analyzer (ESA, Agilent, N9030A



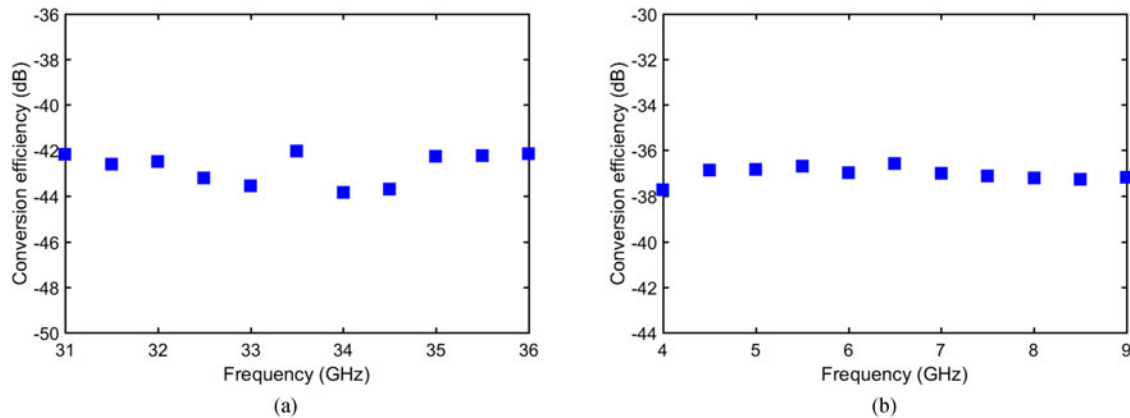


Fig. 6. The conversion efficiency of the proposed microwave photonic mixer in (a) upconversion and (b) downconversion.

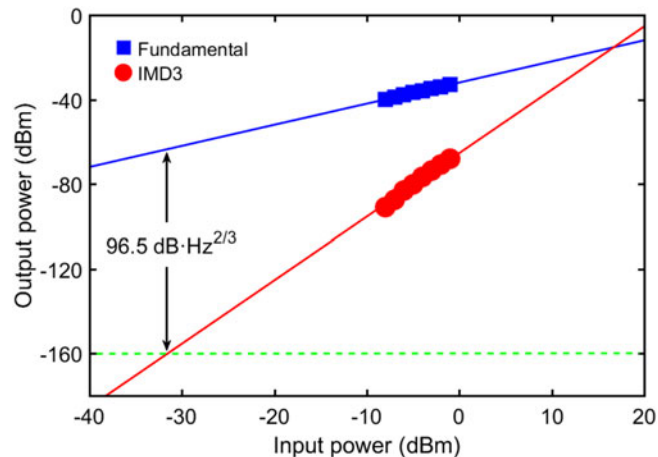


Fig. 7. The SFDR of the proposed microwave photonic mixer.

PXA). The upconverted IF signal is shown in Fig. 5(a), its frequency is 34 GHz and the power is  $-31.8$  dBm. The spur suppression ratio of IF signal is 19.0 dB. In the downconversion case, the frequency and power of IF signal are respectively 6 GHz and  $-27.8$  dBm as depicted in Fig. 5(b). The spur suppression ratio of IF signal is 25.5 dB. Owing to the CS-SSB modulation of RF and LO signals, the high spectral purity of optical sidebands ensures the quality of electrical signals. Although the useless sidebands are well suppressed by adjusting the DC bias voltages of DP-DPMZM, in fact, they cannot be reduced below the noise floor. Therefore, these residual optical sidebands still exist in the passband of OBPF, and several mixing spurs at the frequency of  $\omega_{RF} - \omega_{LO}$  and  $2\omega_{LO}$ , etc., are generated in electrical spectrum.

Finally, the performance of the proposed mixer is analyzed. The conversion efficiency of upconversion and downconversion are measured. The frequency of RF signal is swept from 11 to 16 GHz and the frequency of LO signal is fixed at 10 GHz. The corresponding frequency of upconversion signal is from 31 to 36 GHz. As shown in Fig. 6(a), the conversion efficiency of upconversion is  $-42.7 \pm 0.6$  dB. In the downconversion mode, the frequency of the IF signal is from 9 to 4 GHz. And the conversion efficiency of downconversion is  $-37.0 \pm 0.3$  dB as depicted in Fig. 6(b). It is demonstrated that the conversion efficiency of our system is flat enough in both upconversion and downconversion modes within the bandwidth of 5 GHz. Generally, the power responses of the components used in the link, such as the electrical  $90^\circ$  hybrid coupler, PD, DP-DPMZM and electrical

cable, become worse from low frequency to high frequency. Therefore, the conversion efficiency of upconversion is lower than that of downconversion. To further improve the conversion efficiency of the system, a semiconductor optical amplifier cascaded with an EDFA can be used before PD [21].

For the microwave photonic mixer, spurious-free dynamic range is another important performance parameter. SFDR is the power ratio of the fundamental signal to the third-order intermodulation distortion (IMD3) when the power of IMD3 is equal to the noise floor. The two-tone RF signal with the frequencies of 13.9 and 14 GHz are used to test the SFDR of the system. The power and the frequency of LO signal are 19 dBm and 10 GHz, respectively. The frequencies of the fundamental signals are 6 GHz and 6.1 GHz, and the frequencies of the IMD3 signals are 5.9 GHz and 6.2 GHz. The fundamental and IMD3 signals are measured by ESA, and the results are shown in Fig. 7. If the noise floor of  $-160$  dBm/Hz is supposed, the SFDR of system is  $96.5$  dB $\cdot$ Hz $^{2/3}$ . Although the SFDR is not very high, the proposed mixer can also be used in various civil digital communications. The transmission of digital information has a relatively high noise tolerance, and the SFDR of our proposed mixer is enough for the subsequent signal processing.

#### 4. Conclusion

A microwave photonic mixer based on LO frequency doubling has been theoretically analyzed and experimentally demonstrated. A DP-DPMZM, an electrical  $90^\circ$  hybrid coupler and an OBPF are combined used to generate the CS-SSB modulation of the  $-1$ st-order RF and  $+2$ nd-order LO sidebands. The upconverted IF signal with the frequency of  $\omega_{RF} + 2\omega_{LO}$  is output by a PD. Meanwhile, the  $-1$ st-order RF sideband can be easily changed to  $+1$ st-order RF sideband by adjusting the DC bias voltage of parent MZM in the first sub-DPMZM. The downconverted IF signal with the frequency of  $\omega_{RF} - 2\omega_{LO}$  is obtained correspondingly. The experimental results show that the optical spectrums of both up and downconversion are very pure owing to the optimal design of CS-SSB modulation. Thus, the output electrical spectrums also possess high purity. The spur suppression ratios of upconverted and downconverted IF signal are 19.0 dB and 25.5 dB, respectively. The SFDR of system is  $96.5$  dB $\cdot$ Hz $^{2/3}$ . Since the  $+2$ nd-order LO single sideband is selected, the proposed mixer reduces the frequency requirement of LO signal. Furthermore, the upconversion and downconversion modes can separately operation by a simple electrical switch. The proposed microwave photonic mixer supplies an alternative with high purity and good flexibility for the transmitter and receiver in various civil digital communications.

---

#### References

- [1] R. A. Minasian, E. H. W. Chan, and X. Yi, "Microwave photonic signal processing," *Opt. Exp.*, vol. 21, no. 19, pp. 22918–22936, Sep. 2013.
- [2] J. P. Yao, "Microwave photonics," *J. Lightw. Technol.*, vol. 27, no. 3, pp. 314–335, Feb. 2009.
- [3] J. Capmany and D. Novak, "Microwave photonics combines two worlds," *Nature Photon.*, vol. 1, no. 6, pp. 319–330, Jun. 2007.
- [4] T. Jiang, R. Wu, S. Yu, D. Wang, and W. Gu, "Microwave photonic phase-tunable mixer," *Opt. Exp.*, vol. 25, no. 4, pp. 4519–4527, Feb. 2017.
- [5] G. K. Gopalakrishnan, W. K. Burns, and C. H. Bulmer, "Microwave-optical mixing in LiNbO<sub>3</sub> modulators," *IEEE Trans. Microw. Theory Techn.*, vol. 41, no. 12, pp. 2383–2391, Dec. 1993.
- [6] E. H. W. Chan and R. A. Minasian, "High conversion efficiency microwave photonic mixer based on stimulated Brillouin scattering carrier suppression technique," *Opt. Lett.*, vol. 38, no. 24, pp. 5292–5295, Dec. 2013.
- [7] E. H. W. Chan and R. A. Minasian, "Microwave photonic downconversion using phase modulators in a Sagnac loop interferometer," *IEEE J. Sel. Top. Quantum Electron.*, vol. 19, no. 6, pp. 211–218, Nov./Dec. 2013.
- [8] T. Jiang, S. Yu, Q. Xie, J. Li, and W. Gu, "Photonic downconversion based on optical carrier bidirectional reusing in a phase modulator," *Opt. Lett.*, vol. 39, no. 17, pp. 4990–4993, Sep. 2014.
- [9] Z. Tang, F. Zhang, D. Zhu, X. Zou, and S. Pan, "A photonic frequency downconverter based on a single dual-drive Mach-Zehnder modulator," in *Proc. IEEE Top. Meeting Microw. Photon.*, 2013, pp. 150–153.
- [10] E. H. W. Chan and R. A. Minasian, "Microwave photonic downconverter with high conversion efficiency," *J. Lightw. Technol.*, vol. 30, no. 23, pp. 3580–3585, Dec. 2012.
- [11] Z. Tang and S. Pan, "A reconfigurable photonic microwave mixer," in *Proc. IEEE Int. Top. Meeting Microw. Photon.*, 2014, pp. 343–345.

- [12] H. Li *et al.*, "High dynamic range microwave photonic down-conversion based on dual-parallel Mach–Zehnder modulator," in *Proc. SPIE*, Oct. 2016, vol. 10158, Paper 1015812.
- [13] J. Li *et al.*, "Microwave photonic frequency down-conversion link based on intensity and phase paralleled modulation," in *Proc. SPIE*, Jan. 2017, vol. 10244, Paper 102441O.
- [14] Z. Tang and S. Pan, "A filter-free photonic microwave single sideband mixer," *IEEE Microw. Wireless Compo. Lett.*, vol. 26, no. 1, pp. 67–69, Jan. 2016.
- [15] J. Xu *et al.*, "Microwave photonic frequency downconverter based on single sideband modulation," in *Proc. SPIE*, Oct. 2017, vol. 10464, Paper 104641F.
- [16] Y. Wang *et al.*, "Ultra-wideband microwave photonic frequency downconverter based on carrier-suppressed single-sideband modulation," *Opt. Commun.*, vol. 410, pp. 799–804, Mar. 2018.
- [17] Y. Gao *et al.*, "An efficient photonic mixer with frequency doubling based on a dual-parallel MZM," *Opt. Commun.*, vol. 321, pp. 11–15, Jun. 2014.
- [18] C. Yin *et al.*, "Microwave photonic frequency up-converter with frequency doubling and compensation of chromatic-dispersion-induced power fading," *IEEE Photon. J.*, vol. 9, no. 3, Jun. 2017, Art. no. 5502307.
- [19] H. Chi and J. Yao, "Frequency quadrupling and upconversion in a radio over fiber link," *J. Lightw. Technol.*, vol. 26, no. 15, pp. 2706–2711, Aug. 2008.
- [20] J. Zhang, E. H. W. Chan, X. Wang, X. Feng, and B. Guan, "Broadband microwave photonic sub-harmonic downconverter with phase shifting ability," *IEEE Photon. J.*, vol. 9, no. 3, pp. 1–10, Jun. 2017.
- [21] B. Hraimel *et al.*, "Optical single-sideband modulation with tunable optical carrier to sideband ratio in radio over fiber systems," *J. Lightw. Technol.*, vol. 29, no. 5, pp. 775–781, Mar. 2011.